Stochastic Resonance with Colored Noise for Neural Signal Detection

Fabing Duan[1]*, François Chapeau-Blondeau[2], Derek Abbott[3]

1 Institute of Complexity Science, Qingdao University, Qingdao, P. R. China, **2** Laboratoire d'Ingénierie des Systèmes Automatisés, Université d'Angers, Angers, France, **3** Centre for Biomedical Engineering and School of Electrical & Electronic Engineering, The University of Adelaide, Adelaide, Southern Australia, Australia

Abstract

We analyze signal detection with nonlinear test statistics in the presence of colored noise. In the limits of small signal and weak noise correlation, the optimal test statistic and its performance are derived under general conditions, especially concerning the type of noise. We also analyze, for a threshold nonlinearity–a key component of a neural model, the conditions for noise-enhanced performance, establishing that colored noise is superior to white noise for detection. For a parallel array of nonlinear elements, approximating neurons, we demonstrate even broader conditions allowing noise-enhanced detection, via a form of suprathreshold stochastic resonance.

Citation: Duan F, Chapeau-Blondeau F, Abbott D (2014) Stochastic Resonance with Colored Noise for Neural Signal Detection. PLoS ONE 9(3): e91345. doi:10.1371/journal.pone.0091345

Editor: Maurice J. Chacron, McGill University, Canada

Received November 16, 2013; **Accepted** February 10, 2014; **Published** March 14, 2014

Funding: This work is sponsored by the NSF of Shandong Province (No. ZR2010FM006). The funders had no role in study design, data collection and analysis, decision to publish, or preparation of the manuscript.

Competing Interests: DA is a PLOS ONE Editorial Board member, and the authors here confirm that this does not alter the authors' adherence to all the PLOS ONE policies on sharing data and materials.

* E-mail: fabing.duan@gmail.com

Introduction

Stochastic resonance has emerged as a significant statistical phenomenon where the presence of noise is beneficial for signal and information processing in both man-made and natural systems [1–11]. The excitable FitzHugh–Nagumo (FHN) neuron model has been discussed for exploring the functional role of noise in neural coding of sensory information [12]. Following this, the milestone concept of aperiodic stochastic resonance using the FHN neuron model [13] stimulated a number of interesting investigations in sensory biology [3,7,14,15] and physiological experiments [6,8,16–20]. Due to the character of activity in the nervous system, the neuron coding strategy based on stochastic resonance is also found in threshold (level-crossing) [21–23] and threshold-free [24–28] neurons. Since there are large numbers of neurons in the nervous system of animals and humans with variations in structure, function and size [2,4,7–9], then the potential exploitation of stochastic resonance in a neuron bundle becomes an interesting open question in neuroscience. In a general summing neural network, Collins *et al.* [4] reported that the noise intrinsic to each neuron could be used to extend the operating range of the sensitivity of the overall system. This, however, is not a unique case. In the summing multi-threshold network, suprathreshold stochastic resonance discovered by Stocks [29] overcomes the restriction of subthreshold signals, and appears to offer a possible explantation of dc adaptation in sensory neurons [9,30]. One-dimensional coupling [31] and spatio-temporal stochastic resonance [7,32] show that not only an optimal noise intensity but also an optimal coupling strength exists. Recent stochastic resonance research in complex networks [33–40] also demonstrates that an interconnected network configuration, as well as the non-zero noise level, can be optimized to achieve the best system performance.

In many practical situations, the idealization of white noise is never exactly realized [2,5]. Consequently, the effect of colored noise on stochastic resonance has been investigated using the measure of output signal-to-noise ratio of a periodic signal [2,5,16,41–43]. Although the suppression of stochastic resonance with increasing noise correlation time was demonstrated [2,5,41–43], it is interesting to note that, under certain circumstances, colored noise can be superior to white noise for enhancing the response of a nonlinear system to a weak signal [16,44]. In the field of signal detection, the employment of noise to enhance signal detectability also becomes a possible option [45–55]. However, in most of these studies, the observed noise samples are often assumed to be independent. Colored noise for signal detection [56–60] is not adequately investigated in the context of stochastic resonance. In this article, we focus on the weak signal detection problem with the beneficial role of additive colored noise in threshold neurons. Because of the "all-and-none" character of nerve activity [61], the problem of threshold-based neural signal detection can be considered as a statistical binary hypothesis test [7,23,27]. In this situation, explicit expressions for the maximum asymptotic detection efficacy are derived for a given transfer function of neuron model. We prove that colored noise that arises from a moving-average model is superior to white noise in improving the detection efficacy of neurons. It is illustratively shown that, for a single neuron with a signum threshold nonlinearity, the possibility of noise-enhanced detection only holds for non-scaled noise. For scaled noise, the effect of noise-enhanced detection does not occur in a single neuron model. However, when we tune the internal noise components of a parallel array of threshold neurons, it is observed that the constructive role of noise comes into play again in improving the signal detection efficacy, wherein suprathreshold stochastic resonance manifests its potentiality.

Results

Detection model

Consider the detection problem formulated as a binary hypothesis test [23,60,62]

$$\begin{aligned} H_0 &: \mathbf{x}=\mathbf{z}, \\ H_1 &: \mathbf{x}=\mathbf{z}+\theta\mathbf{s}. \end{aligned} \tag{1}$$

Under hypothesis H_0, the observation vector $\mathbf{x}=[x_1,x_2,\cdots,x_N]^T$ consists of noise $\mathbf{z}=[z_1,z_2,\cdots,z_N]^T$ only, and under hypothesis H_1 it consists of noise $\mathbf{z}$ and known signal $\mathbf{s}=[s_1,s_2,\cdots,s_N]^T$ with its strength θ. There exists a finite bound U_s such that $0\leq|s_n|\leq U_s$, and the asymptotic average signal power satisfies $0<P_s=\lim_{N\to\infty}\mathbf{s}^T\mathbf{s}/N<\infty$ [56–58,60,62]. Next, the test statistic $T(\mathbf{x})$ is compared with a decision threshold γ to decide the hypotheses, as

$$T(\mathbf{x})=\mathbf{c}^T g(\mathbf{x}) \underset{H_0}{\overset{H_1}{\gtrless}} \gamma, \tag{2}$$

where the coefficient vector $\mathbf{c}=[c_1,c_2,\cdots,c_N]^T$ is associated with the function $g(\mathbf{x})$ to form $T(\mathbf{x})$.

Assume the N-dimensional probability distribution $f(\mathbf{z})$ of noise $\mathbf{z}$ and zero-mean vector of $\mathrm{E}[g(\mathbf{z})]=\int g(\mathbf{z})f(\mathbf{z})d\mathbf{z}$ (for a shift in mean) [58,60]. Then, for a large sample size N of observation vector $\mathbf{x}$, the test statistic $T(\mathbf{x})$ has zero-mean and asymptotic variance

$$\mathrm{var}(T(\mathbf{x})|H_0)=\mathbf{c}^T\mathrm{E}[g(\mathbf{z})g(\mathbf{z})^T]\mathbf{c}, \tag{3}$$

under hypothesis H_0. Furthermore, for weak signals ($\theta\to 0$) and under hypothesis H_1, $g(\mathbf{x})$ can be expanded to the first-order

$$g(\mathbf{x})=g(\mathbf{z}+\theta\mathbf{s})\approx g(\mathbf{z})+\theta\frac{\partial g(\mathbf{z})}{\partial\mathbf{z}}\ \mathbf{s}. \tag{4}$$

Then, the characteristics of $T(\mathbf{x})$ under H_1, up to the first-order in θ, can be calculated as

$$\mathrm{E}(T(\mathbf{x})|H_1)\approx\theta\mathbf{c}^T\mathrm{E}[\frac{\partial g(\mathbf{z})}{\partial\mathbf{z}}]\mathbf{s},\ \ \mathrm{var}(T(\mathbf{x})|H_1)\approx\mathrm{var}(T(\mathbf{x})|H_0). \tag{5}$$

Under both hypotheses H_0 and H_1, the test statistic $T(\mathbf{x})$, according to the central limit theorem, converges to a Gaussian distribution. Thus, the binary hypothesis test of Eq. (1) becomes a Gaussian mean-shift detection problem [60,62]. Given the false probability, the detection probability is a monotonically increasing function of the detection efficacy $\xi(T)$ [60,62] given by

$$\begin{aligned} \xi(T) &= \lim_{N\to\infty}\frac{\left(\partial\mathrm{E}[T(\mathbf{x})|H_1]/\partial\theta|_{\theta=0}\right)^2}{\mathrm{var}[T(\mathbf{x})|H_0]} \\ &= \frac{(\mathbf{c}^T\mathrm{E}[\partial g(\mathbf{z})/\partial\mathbf{z}]\mathbf{s})^2}{\mathbf{c}^T\mathrm{E}[g(\mathbf{z})g^T(\mathbf{z})]\mathbf{c}} \\ &= \frac{\left(\mathbf{c}^T\mathrm{E}[g(\mathbf{z})(\partial\ln f(\mathbf{z})/\partial\mathbf{z})^T]\mathbf{s}\right)^2}{\mathbf{c}^T\mathrm{E}[g(\mathbf{z})g(\mathbf{z})^T]\mathbf{c}} \\ &\leq \mathbf{s}^T\mathbf{J}\ \mathbf{s}, \end{aligned} \tag{6}$$

where the Cauchy-Schwarz inequality yields

$$\left(\mathbf{c}^T\mathrm{E}[g(\mathbf{z})(\frac{\partial\ln f(\mathbf{z})}{\partial\mathbf{z}})^T]\mathbf{s}\right)^2\leq\mathbf{c}^T\mathrm{E}[g(\mathbf{z})g(\mathbf{z})^T]\mathbf{c}\cdot\mathbf{s}^T\mathbf{J}\ \mathbf{s}, \tag{7}$$

with the Fisher information matrix $\mathbf{J}=\mathrm{E}[(\frac{\partial\ln f(\mathbf{z})}{\partial\mathbf{z}})(\frac{\partial\ln f(\mathbf{z})}{\partial\mathbf{z}})^T]$. Note that the equality of Eq. (6) is satisfied by the locally optimum nonlinearity

$$g_{\mathrm{opt}}(\mathbf{z})=C\frac{\partial\ln f(\mathbf{z})}{\partial\mathbf{z}}, \tag{8}$$

for an arbitrary constant C.

However, a complete closed-form noise distribution $f(\mathbf{z})$ may be unavailable, especially in unknown noisy circumstances [56–58,60,62], which makes the nonlinearity of Eq. (8) difficult or too complex to implement. Thus, there may be compelling reasons for considering the given function g with an easily implemented feature. In this case, the detection efficacy in Eq. (6) can be maximized as

$$\begin{aligned} \xi(T) &= \frac{(\mathbf{c}^T\mathrm{E}[\partial g(\mathbf{z})/\partial\mathbf{z}]\mathbf{s})^2}{\mathbf{c}^T\mathrm{E}[g(\mathbf{z})g^T(\mathbf{z})]\mathbf{c}} \\ &= \frac{\left[\left(\mathbf{L}^T\mathbf{c}\right)^T\left(\mathbf{L}^{-1}\mathrm{E}[\partial g(\mathbf{z})/\partial\mathbf{z}]\mathbf{s}\right)\right]^2}{\left(\mathbf{L}^T\mathbf{c}\right)^T\left(\mathbf{L}^T\mathbf{c}\right)} \\ &\leq \mathbf{s}^T\mathrm{E}\left[\frac{\partial g(\mathbf{z})}{\partial\mathbf{z}}\right]^T\mathbf{V}^{-1}\mathrm{E}\left[\frac{\partial g(\mathbf{z})}{\partial\mathbf{z}}\right]\mathbf{s}, \end{aligned} \tag{9}$$

with the Cholesky decomposition of the variance matrix $\mathbf{V}=\mathrm{E}\left[g(\mathbf{z})g(\mathbf{z})^T\right]=\mathbf{L}\mathbf{L}^T$ and by optimally choosing the coefficient vector $\mathbf{c}_{\mathrm{opt}}=\kappa\ \mathrm{E}[g(\mathbf{z})g(\mathbf{z})^T]^{-1}\mathrm{E}[\partial g(\mathbf{z})/\partial\mathbf{z}]\mathbf{s}$ for an arbitrary constant κ.

Colored noise

Consider a useful colored noise model of the first-order moving-average [56,59] as

$$z_i=\rho_1 w_{i-1}+w_i+\rho_2 w_{i+1}, \tag{10}$$

where the correlation coefficients are $\rho_{1,2}$ and $\mathbf{w}=[w_1,w_2,\cdots,w_N]^T$ is an independent identically distributed (i.i.d.) random vector. For small values of $\rho_{1,2}$ ($|\rho_{1,2}|\ll 1$), the dependence among noise samples z_i will be weak [56,59]. Here, we assume w_i have an univariate distribution $f_w(w)$ that is symmetric about the origin. We also assume the memoryless nonlinearity $g(\mathbf{z})=[g(z_1),g(z_2),\cdots,g(z_N)]^T$ to be odd symmetric about the origin. Then, up to first order in small correlation coefficients $\rho_{1,2}$, we can expand $g(z_i)$ as

$$g(z_i)\approx g(w_i)+(\rho_1 w_{i-1}+\rho_2 w_{i+1})g'(w_i), \tag{11}$$

$$g'(z_i)\approx g'(w_i)+(\rho_1 w_{i-1}+\rho_2 w_{i+1})g''(w_i), \tag{12}$$

and obtain expectations

$$\mathrm{E}[g'(z_i)]\approx\mathrm{E}[g'(w)], \tag{13}$$

$$\mathrm{E}[g^2(z_i)] \approx \mathrm{E}[g^2(w)], \tag{14}$$

$$\mathrm{E}[g(z_i)g(z_{i+1})] \approx (\rho_1+\rho_2)\mathrm{E}[wg(w)]\mathrm{E}[g'(w)]. \tag{15}$$

Therefore, we have the expectation matrix

$$\mathrm{E}\left[\frac{\partial g(\mathbf{z})}{\partial \mathbf{z}}\right] \approx \mathrm{E}[g'(w)]\ \mathbf{I}, \tag{16}$$

with the unit matrix $\mathbf{I}$, and the variance matrix $\mathbf{V} = \mathrm{E}\left[g(\mathbf{z})g(\mathbf{z})^T\right]$ has elements

$$\mathbf{V}_{i,i} = \mathrm{E}[g^2(w)], \tag{17}$$

$$\mathbf{V}_{i,i+1} = \mathbf{V}_{i+1,i} = (\rho_1+\rho_2)\mathrm{E}[wg(w)]\mathrm{E}[g'(w)], \tag{18}$$

for $i=1,2,\cdots,N$. Then, based on Eq. (9), the normalized detection efficacy $e(g)$ can be computed as

$$\begin{aligned} e(g,\rho) &= \frac{\xi(T)}{NP_s} \\ &= \frac{\mathbf{s}^T\mathrm{E}[\partial g(\mathbf{z})/\partial\mathbf{z}]^T\mathbf{V}^{-1}\mathrm{E}[\partial g(\mathbf{z})/\partial\mathbf{z}]\mathbf{s}}{\mathbf{s}^T\mathbf{s}} \\ &= \mathrm{E}^2[g'(w)]\ \frac{\mathbf{s}^T\mathbf{V}^{-1}\mathbf{s}}{\mathbf{s}^T\mathbf{s}} \\ &\le \frac{\mathrm{E}^2[g'(w)]}{\lambda_{\min}}. \end{aligned} \tag{19}$$

Here, when the equality of Eq. (19) is achieved, the signal $\mathbf{s}$ is the corresponding eigenvector to the minimum eigenvalue $\lambda_{\min}$ of the matrix $\mathbf{V}$. It is known that the eigenvalues of the matrix $\mathbf{V}$ are [62]

$$\begin{aligned} \lambda_i &= \mathbf{V}_{i,i} + 2\mathbf{V}_{i,i+1}\cos\left(\frac{\pi i}{N+1}\right) \\ &= \mathrm{E}[g^2(w)] + 2(\rho_1+\rho_2)\mathrm{E}[wg(w)]\mathrm{E}[g'(w)]\cos\left(\frac{\pi i}{N+1}\right), \end{aligned} \tag{20}$$

corresponding to eigenvectors $\mathbf{v}_i = \sin(\pi ik/(N+1))$ for $k=1,2,\cdots,N$. Here, as the nonlinearity g is assumed to be odd, it is then found that $\mathrm{E}[wg(w)] \ge 0$ and $\mathrm{E}[g'(w)] \ge 0$. Therefore, if $\rho_1+\rho_2<0$ and for a large sample size N, we take $i=1$ and $\lambda_{\min}=\lambda_1 \approx \mathrm{E}[g^2(w)] + 2(\rho_1+\rho_2)\mathrm{E}[wg(w)]\mathrm{E}[g'(w)]$. Otherwise, we choose $\lambda_{\min}=\lambda_N \approx \mathrm{E}[g^2(w)] - 2(\rho_1+\rho_2)\mathrm{E}[wg(w)]\mathrm{E}[g'(w)]$. An illustration of the eigenvector $\mathbf{v}_N$ is shown in Fig. 1 for $N=200$. In this way, by optimally choosing the input signal (eigenvector) $\mathbf{s}=\mathbf{v}_1$ ($\mathbf{v}_N$), the maximum efficacy $e(g,\rho)$ can be calculated as

$$\begin{aligned} e_{\max}(g,\rho) &= \max_{\mathbf{s}}\ e(g,\rho) \\ &= \frac{\mathrm{E}^2[g'(w)]}{\mathbf{V}_{i,i} - 2|\mathbf{V}_{i,i+1}|} \\ &= \frac{\mathrm{E}^2[g'(w)]}{\mathrm{E}[g^2(w)] - 2|\rho_1+\rho_2|\ \mathrm{E}[wg(w)]\ \mathrm{E}[g'(w)]}. \end{aligned} \tag{21}$$

Since, from its definition in Eq. (6), the efficacy $e(g,\rho)$ is non-negative, the denominator in Eq. (21) must satisfy

$$\mathrm{E}[g^2(w)] - 2|\rho_1+\rho_2|\mathrm{E}[wg(w)]\mathrm{E}[g'(w)] > 0. \tag{22}$$

In order to validate Eq. (22), we use the Cauchy-Schwarz inequality to yield

$$\mathrm{E}^2[wg(w)] \le \mathrm{E}[w^2]\mathrm{E}[g^2(w)] = \sigma_w^2\mathrm{E}[g^2(w)], \tag{23}$$

$$\mathrm{E}^2[g'(w)] \le \mathrm{E}[(\frac{f_w'}{f_w})^2]\mathrm{E}[g^2(w)] = J(f_w)\mathrm{E}[g^2(w)], \tag{24}$$

with the Fisher information quantity $J(f_w) = \mathrm{E}[(f_w'/f_w)^2]$ and the variance σ_w^2 of noise distribution of f_w [56]. Thus, we find

$$\mathrm{E}[wg(w)]\ \mathrm{E}[g'(w)] \le \sqrt{\sigma_w^2 J(f_w)}\ \mathrm{E}[g^2(w)]. \tag{25}$$

Substituting Eq. (25) into Eq. (22) and noting

$$\sigma_w^2 J(f_w) = \mathrm{E}[w^2]\mathrm{E}\left[\left(\frac{f_w'}{f_w}\right)^2\right] \ge \mathrm{E}\left[w\frac{f_w'}{f_w}\right]^2 = 1, \tag{26}$$

we have

$$|\rho_1+\rho_2| \le \frac{1}{2\sqrt{\sigma_w^2 J(f_w)}} \le \frac{1}{2}. \tag{27}$$

Since we assume $|\rho_{1,2}| \ll 1$, the inequalities of Eqs. (27) and (22) can be satisfied, and the detector efficacy in Eq. (21) will be theoretically analyzed in the following.

For white noise vector $\mathbf{z}$ with zero correlation coefficients $\rho_{1,2}=0$, the detection efficacy $e(g,\rho)$ in Eq. (21) satisfies

$$e(g,\rho) = \frac{\mathrm{E}^2[g'(w)]}{\mathrm{E}[g^2(w)]} \le e_{\max}(g,\rho). \tag{28}$$

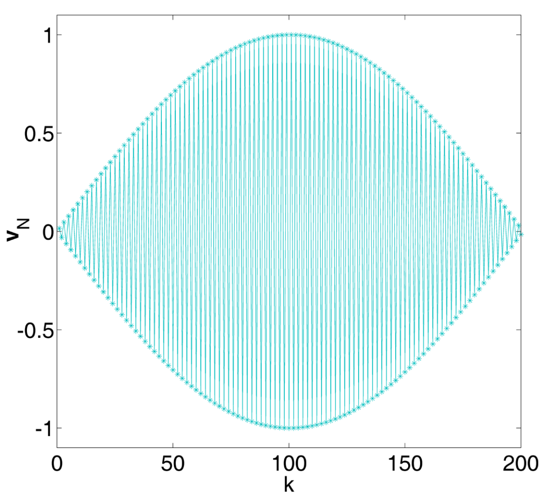

Figure 1. Eigenvector $\mathbf{v}_N$**.** An illustration of the eigenvector $\mathbf{v}_N$ of the variance matrix $\mathbf{V}$ ($N=200$).
doi:10.1371/journal.pone.0091345.g001

Thus, for a given function g, colored noise is superior to white noise in enhancing the detection efficacy, at a cost of optimally matching the input signal with the eigenvector $\mathbf{v}_i$ of covariance matrix $\mathbf{V}$.

Stochastic resonance in threshold-based neurons

We will illustratively show the possibilities of noise-enhanced detection in threshold-based neurons. The classical McCulloch-Pitts threshold neuron has the form

$$g(x)=\begin{cases}1, x>\ell,\\ 0, x\le\ell,\end{cases} \tag{29}$$

with the response threshold ℓ. It is seen that g can be expressed as a function of x in terms of the signum (sign) function as $g(x)=\frac{1}{2}\mathrm{sign}(x-\ell)+\frac{1}{2}$. Since the constant factor $1/2$ does not affect the detection efficacy of the transfer function g, then we focus on the signum function

$$g(x)=\mathrm{sign}(x), \tag{30}$$

with response threshold $\ell=0$ in the following parts. Here, the signum function g is not continuous at $x=0$, but has its derivative $g'(x)=2\delta(x)$ for any x [60].

For the colored noise model of Eq. (10), the correlation coefficient $\rho_2=0$ indicates the noise sequence z_i is a causal process that can be physically realized. Here, we assume $\rho_1=\rho$ ($|\rho|\ll 1$) and $\rho_2=0$, and show the possibility of stochastic resonance in the physically realizable noise environment. First, consider scaled noise $w(t)=\sigma_w w_0(t)$ that has the distribution $f_w(w)=f_{w_0}(w/\sigma_w)/\sigma_w$ [23,60]. Here, $w_0(t)$ has a standardized distribution f_{w_0} with unity variance $\sigma_{w_0}^2=1$. Thus, based on Eq. (21), the absolute moment is

$$\mathrm{E}[wg(w)]=\mathrm{E}[w\,\mathrm{sign}(w)]=\mathrm{E}[|w|]=\sigma_w \mathrm{E}_{w_0}[|w_0|], \tag{31}$$

where the operator $\mathrm{E}_{w_0}[\cdot]=\int \cdot f_{w_0}(w_0)dw_0$. Thus, for the signum function g, the detection efficacy of Eq. (21) can be expressed as

$$e_{\max}(g,\rho)=\frac{4f_w^2(0)}{1-4|\rho|f_w(0)\mathrm{E}[|w|]}=\frac{4\sigma_w^{-2}f_{w_0}^2(0)}{1-4|\rho|f_{w_0}(0)\mathrm{E}_{w_0}[|w_0|]}. \tag{32}$$

It is seen in Eq. (32) that $e_{\max}(g,\rho)$ is a monotonically decreasing function of noise variance σ_w^2, and no noise-enhanced detection effect will occur in such a single neuron model for scaled noise.

We further consider non-scaled Gaussian mixture distribution [5,47,48,60]

$$f_w(x)=\frac{1}{2\sqrt{2\pi\epsilon^2}}\left[\exp\left(\frac{-(x-\mu)^2}{2\epsilon^2}\right)+\exp\left(\frac{-(x+\mu)^2}{2\epsilon^2}\right)\right], \tag{33}$$

where the variance $\sigma_w^2=\mu^2+\epsilon^2$ and parameters $\mu,\epsilon\ge 0$. Then, for the signum function g in Eq. (30), the detection efficacy of Eq. (21) can be computed as

$$e_{\max}(g,\rho)=\frac{\frac{2}{\pi\epsilon^2}\exp\left(-\frac{\mu^2}{\epsilon^2}\right)}{1-2|\rho|\left[\frac{2}{\pi}\exp\left(-\frac{\mu^2}{\epsilon^2}\right)+\sqrt{\frac{2}{\pi}}\frac{\mu}{\epsilon}\exp\left(-\frac{\mu^2}{2\epsilon^2}\right)\mathrm{erf}\left(\frac{\mu}{\sqrt{2}\epsilon}\right)\right]}, \tag{34}$$

where the error function $\mathrm{erf}(x)=2/\sqrt{\pi}\int_0^x \exp(-t^2)dt$. In Fig. 2, for the correlation coefficient $|\rho|=0.2$ and different values of $\mu=0.3, 0.5$ and 1, we show the detection efficacy of Eq. (34) as a function of noise variance σ_w^2. For a given non-zero value μ and as $\epsilon\to 0$, the noise distribution model of Eq. (33) indicates the dichotomous noise [5,48,53]. In this situation, as the signal strength $\theta\to 0$ and $|\theta s_n|\ll\mu$, the signum function g will not change its output whether the signal appears or not. Therefore, the test statistics $T(\mathbf{x})=\mathbf{c}^T g(\mathbf{x})$ in Eq. (2) will be the same value under hypotheses H_0 and H_1, and the detection efficacy $e_{\max}(g,\rho)$ in Eq. (34) starts from zero. This explantation can be also validated by Eq. (34) as $\epsilon\to 0$ and μ being fixed, as illustrated in Fig. 2. However, it is clearly seen that, upon increasing the noise variance $\sigma_w^2=\epsilon^2+\mu^2$ (actually increasing ϵ), the noise-enhanced detection effect appears. The smaller the parameter μ is, the more pronounced the resonant peak of $e_{\max}(g,\rho)$ becomes, as shown in Fig. 2.

Next, an interesting problem is that, for scaled noise, can we observe the noise-enhanced detection effect in threshold-based neurons? The answer to this question is affirmative. Here, we will resort to the constructive role of internal noise for improving the performance of an array of threshold neurons. Let $\bar{\mathbf{x}}_m=[\bar{x}_{1,m},\bar{x}_{2,m},\cdots,\bar{x}_{N,m}]^T$ be the vector of N observation components at the m-th element of receiving array of M identical neurons. In this observation model, $\bar{x}_{i,m}=z_i+y_{i,m}$ under the hypothesis H_0. Here, in each neuron element, the M noise terms y_m are assumed to be mutually independent with the same PDF f_y and variance σ_y^2. Then, at the observed time i, the array outputs are collected as $\bar{g}(\bar{x}_i)=\sum_{m=1}^M g(\bar{x}_{i,m})/M$, and the test statistics can be reconstructed as $T_{\mathrm{GC}}(\bar{\mathbf{x}})=\mathbf{c}^T\bar{g}(\bar{\mathbf{x}})$ with $\bar{g}(\bar{\mathbf{x}})=[\bar{g}(\bar{x}_1),\bar{g}(\bar{x}_2),\cdots,\bar{g}(\bar{x}_N)]^T$. For the colored noise model of Eq. (10) with $\rho_1=\rho$ and $\rho_2=0$, we have

$$g(\bar{x}_i)\approx g(v_i)+\rho w_{i-1}g'(v_i), \tag{35}$$

$$g'(\bar{x}_i)\approx g'(v_i)+\rho w_{i-1}g''(v_i), \tag{36}$$

where the composite noise $v_i=w_i+y_i$ has the convolved distribution $f_v(v)=\int f_w(v-u)f_y(u)du$. Then, we have expectations

$$\mathrm{E}_v[\bar{g}'(\bar{x}_i)]=\frac{1}{M}\sum_{m=1}^M \mathrm{E}_v[g'(\bar{x}_{i,m})]\approx \mathrm{E}_v[g'(v)], \tag{37}$$

and

$$\mathrm{E}_v\left[\frac{\partial\bar{g}(\bar{\mathbf{x}})}{\partial\bar{\mathbf{x}}}\right]\approx \mathrm{E}_v[g'(v)]\,\mathbf{I}, \tag{38}$$

with the operator $\mathrm{E}_v[\cdot]=\int\cdot f_v(v)dv$. The variance matrix $\bar{\mathbf{V}}=\mathrm{E}_v\left[\bar{g}(\bar{\mathbf{x}})\bar{g}(\bar{\mathbf{x}})^T\right]$ has elements

$$\begin{aligned}\bar{\mathbf{V}}_{i,i}&=\mathrm{E}_v[\bar{g}^2(\bar{x}_i)]\\ &=\mathrm{E}_w\left\{\frac{1}{M^2}\sum_{m=1}^M\sum_{n=1}^M \mathrm{E}_y[g(\bar{x}_{i,m})g(\bar{x}_{i,n})]\right\}\\ &\approx\frac{1}{M}\mathrm{E}_v[g^2(v)]+\frac{(M-1)}{M}\mathrm{E}_w\{\mathrm{E}_y^2[g(w+y)]\},\end{aligned} \tag{39}$$

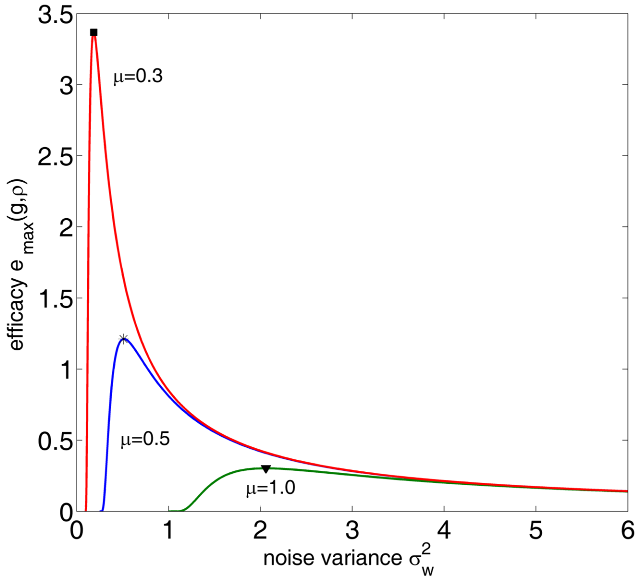

Figure 2. Stochastic resonance of a single threshold neuron. Detection efficacy of $e_{\max}(g,\rho)$ as a function of noise variance $\sigma_w^2=\mu^2+\epsilon^2$ for the correlation coefficient $|\rho|=0.2$ and different values of $\mu=0.3$ (red), 0.5 (blue) and 1 (green). The resonant peaks of $e_{\max}(g,\rho)$ are marked by the square (■), the star (∗) and the down triangle (▼) for $\mu=0.3,0.5$ and 1, respectively. Here, the transfer function $g(x)=\text{sign}(x)$, and the noise distribution is Gaussian mixture model of Eq. (33).
doi:10.1371/journal.pone.0091345.g002

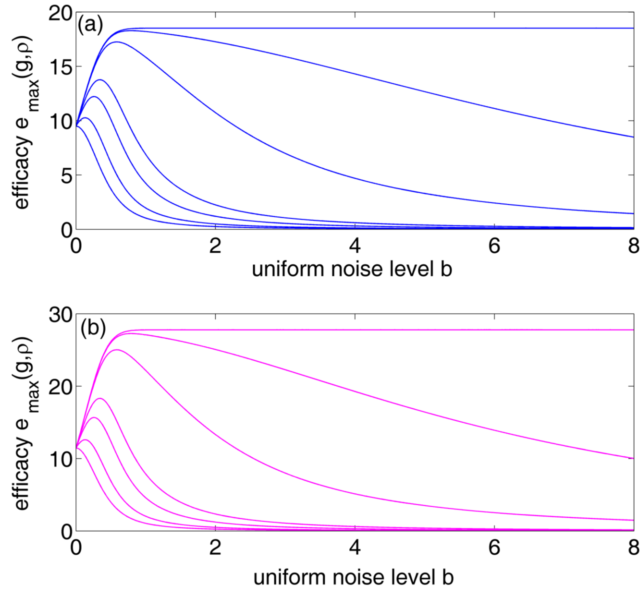

Figure 3. Suprathreshold stochastic resonance in an array of threshold neurons. Detection efficacy $e_{\max}(g,\rho)$ as a function of the internal uniform noise level b and the neuron array size M. From the bottom upwards, $M=1,2,5,10,100,1000,\infty$. Here, the initial Gaussian noise level $\sigma_w=0.3$, the transfer function $g(x)=\text{sign}(x)$, the correlation coefficient (a) $|\rho|=0.2$ and (b) $|\rho|=0.3$.
doi:10.1371/journal.pone.0091345.g003

$$\begin{aligned}\overline{\mathbf{V}}_{i,i+1}=\overline{\mathbf{V}}_{i+1,i}&=\mathrm{E}_v[\bar{g}(\bar{x}_i)\bar{g}(\bar{x}_{i+1})]\\&=\mathrm{E}_w\left\{\frac{1}{M^2}\sum_{m=1}^{M}\sum_{n=1}^{M}\mathrm{E}_y[g(\bar{x}_{i,m})g(\bar{x}_{i+1,n})]\right\}\\&=\frac{1}{M^2}\mathrm{E}_w\{M^2\mathrm{E}_y[g(\bar{x}_i)g(\bar{x}_{i+1})]\}\\&\approx\rho\mathrm{E}_w\{w\mathrm{E}_y[g(w+y)]\}\mathrm{E}_v[g'(v)].\end{aligned}\quad(40)$$

Then, based on Eqs. (38), (39) and (40), the maximum efficacy $e_{\max}(g,\rho)$ can be computed by Eq. (21) as

$$e_{\max}(g,\rho)=\max_{\mathbf{s}}\ e(g,\rho)=\frac{\mathrm{E}_v^2[g'(v)]}{\overline{\mathbf{V}}_{i,i}-2|\overline{\mathbf{V}}_{i,i+1}|}.\quad(41)$$

For instance, we assume the initial Gaussian noise components w_i have the distribution of $f_w(x)=\frac{1}{\sqrt{2\pi\sigma_w^2}}\exp\left(-\frac{w^2}{2\sigma_x^2}\right)$ and the given variance σ_w^2. The internal noise components of each neuron is assumed to be the uniform random variable y_i with its distribution $f_y(x)=1/(2b)$ for $-b\le x\le b$ and zero otherwise. The composite random variables v_i are distributed by

$$f_v(x)=\frac{\mathrm{erf}\left(\frac{x+b}{\sqrt{2}\sigma_w}\right)-\mathrm{erf}\left(\frac{x-b}{\sqrt{2}\sigma_w}\right)}{4b}.\quad(42)$$

For a given Gaussian noise level $\sigma_w=0.3$, it is shown in Figs. 3 (a) and (b) that the maximum detection efficacy $e_{\max}(g,\rho)$ varies as a function of internal uniform noise level b for different array sizes M and correlation coefficients ρ. It is noted that, at the uniform noise level $b=0$, the detection efficacy in Eq. (41) is just the expression of Eq. (32) for a single neuron. Thus, $e_{\max}(g,\rho)=9.49$ and 11.45 for $|\rho|=0.2$ (see Fig. 3 (a)) and $|\rho|=0.3$ (see Fig. 3 (b)), respectively. By comparing Fig. 3 (a) with Fig. 3 (b), it is seen that the maximum detection efficacy $e_{\max}(g,\rho)$ can be further enhanced for a higher value of ρ. For the array size $M=1$ and upon increasing uniform noise level b, it is seen in Fig. 3 that there is no noise-enhanced effect in a single neuron. However, as $M\ge 2$, it is illustrated in Fig. 3 that the internal uniform noise can enhance the detection efficacy $e_{\max}(g,\rho)$, and the noise-enhanced effect does occur. Moreover, as the array size M increases, the noise-induced enhancement becomes more visible by adopting an appropriate amount of uniform noise of the neuron array, as shown in Fig. 3. As the detection problem so far is confined to the weak signal with its strength $\theta\to 0$ but $\theta>0$, and the response threshold ℓ of all neurons is zero, thus Fig. 3 shows the potential capability of suprathreshold stochastic resonance in improving the detection efficacy of a parallel array threshold-based neurons.

Methods

Under the assumption of weak signals, the Taylor expansion of the function is utilized in Eqs. (4), (5), (11) and (12). The Cauchy-Schwarz inequality is used in Eqs. (7), (9), (23), and (24). The maximum of Rayleigh quotients for a symmetric matrix is calculated in Eqs. (19), (21) and (41).

Conclusion

In this paper, we study the performance enhancement of threshold-based neurons for detecting weak signals in the presence of colored noise. For a given transfer function, we maximize the detection efficacy by optimally choosing the signal waveform. We prove that colored noise is superior to white noise in enhancing the detection efficacy, at a cost of optimally matching the input signal with the eigenvector of the covariance matrix. Furthermore, we illustrate that, for a single threshold neuron, the possibility of noise-enhanced detection cannot occur in scaled noise, but does appear in a non-scaled Gaussian mixture noise model. Furthermore, for scaled noise, we can test a parallel bundle of neurons with the same response threshold, and recover the positive role of internal noise in enhancing the detection efficacy of the neuron array via the mechanism of suprathreshold stochastic resonance. These results demonstrate that the strategy of exploiting stochastic resonance is still interesting in the case of improving the nonlinear system performance by adding more noise to the signal corrupted by colored noise.

Here, we mainly consider the first-order moving-average noise model of Eq. (10) which is, as we show, amenable to analytical treatment. It is possible to extend the present approach to higher-order moving-average noise models. However, the same analytical treatment maybe no longer feasible. It is also interesting to consider yet other models of colored noise to enhance the detectability of the neuron array. This subject is very promising and currently under study.

It is noted that the detection efficacy of Eqs. (6) and (9) are established under the assumption of weak signal strength $\theta \to 0$. We only consider the first-order Taylor expansion of nonlinearities in Eq. (4), because it makes an analytical treatment possible and the corresponding results are rigorous. In practice, most noise distributions are symmetric and the nonlinear characteristics are odd symmetric about the origin. In this case, we can expand the nonlinearity to the second-order terms. The expectation of the second-order term of Taylor expansion of Eq. (4) vanishes and does not affect the conclusion of this paper. However, for unsymmetrical noise distributions and nonlinearities, the high-order terms of Taylor expansion of Eq. (4) are not exactly zero. For this case, we need to numerically observe the effect of high-order terms on the detector performance. It is interesting to compare the present theoretical results of first-order expansion with the numerical results in the further studies.

We also note that these equations of Eqs. (4)–(9) are the extension of white noise [54,56–58,60] to the case of colored noise. Then, we consider a model of colored noise allowing for an analytical evaluation of the detection efficacy in Eqs. (6) and (9). The detection efficacy can also be numerically computed to address other models of colored noise, or to explore broader conditions beyond the weak signal limit. As the signal strength θ increases, the Taylor expansion of Eq. (4) and the upper bound of Eq. (6) gradually cease to apply. However, based on the present results on weak signal in colored noise, and on [25,26,63] on non-weak signal in Gaussian white noise, it can be expected that noise benefit as reported here will persist with colored noise beyond the small-signal limit.

Author Contributions

Conceived and designed the experiments: FCB DA. Performed the experiments: FD. Analyzed the data: FD FCB DA. Contributed reagents/materials/analysis tools: FCB DA. Wrote the paper: FD FCB DA. Proofreading: FCB DA.

References

1. Benzi R, Sutera A, Vulpiani A (1981) The mechanism of stochastic resonance. Journal of Physics A: Mathematical and General 14: L453–L457.
2. Gammaitoni L, Hänggi P, Jung P, Marchesoni F (1998) Stochastic resonance. Reviews of Modern Physics 70: 233–287.
3. Wiesenfeld K, Moss F (1995) Stochastic resonance and the benefits of noise: from ice ages to crayfish and squids. Nature 373: 33–36.
4. Collins JJ, Chow CC, Imhoff TT (1995) Stochastic resonance without tuning. Nature 376: 236–238.
5. Chapeau-Blondeau F, Godivier X (1997) Theory of stochastic resonance in signal transimission by static nonlinear systems. Physical Review E 55: 1478–1495.
6. Russell DF, Wilkens LA, Moss F (1999) Use of behavioural stochastic resonance by paddle fish for feeding. Nature 401: 291–294.
7. Lindner B, García J, Neiman A, Schimansky-Geier L (2004) Effects of noise in excitable systems. Physics Reports 392: 321–424.
8. Moss F, Ward LM, Sannita WG (2004) Stochastic resonance and sensory information processing: a tutorial and review of application. Clinical NeuroPhysiology 115: 267–281.
9. McDonnell MD, Stocks NG, Pearce CEM, Abbott D (2008) Stochastic resonance: from suprathreshold stochastic resonance to stochastic signal quantization. Cambridge: Cambridge University Press.
10. McDonnell MD, Abbott D (2009) What is stochastic resonance? definitions, misconceptions, debates, and its relevance to biology. PLoS Computational Biology 5: no. e1000348.
11. Ward LM, MacLean SE, Kirschner A (2010) Stochastic resonance modulates neural synchronization within and between cortical sources. PLoS ONE 5: no.e14371.
12. Longtin A (1993) Stochastic resonance in neuron models. Journal of Statistical Physics 70: 309–327.
13. Collins JJ, Chow CC, Imhoff TT (1995) Aperiodic stochastic resonance in excitable systems. Physical Review E 52: R3321–R3324.
14. Bezrukov SM, Vodyanoy I (1995) Noise-induced enhancement of signal transduction across voltagedependent ion channels. Nature 378: 362–364.
15. Levin JE, Miller JP (1996) Broadband neural encoding in the cricket cercal sensory system enhanced by stochastic resonance. Nature 380: 165–168.
16. Nozaki D, Mar DJ, Grigg P, Collins JJ (1999) Effects of colored noise on stochastic resonance in sensory neurons. Physical Review Letters 82: 2402–2405.
17. Collins JJ, Priplata AA, Gravelle DD, Niemi J, Harry J, et al. (2003) Noise-enhanced human sensorimotor function. IEEE Engineering in Medicine and Biology 22: 76–83.
18. Priplata AA, Patritti BL, Niemi JB, Hughes R (2006) Noise-enhanced balance control in patients with diabetes and patients with stroke. Annals of Neurology 59: 4–12.
19. Kitajo K, Yamanaka K, Ward LM (2006) Stochastic resonance in attention control. Europhysics Letters 76: 1029.
20. Kurita Y, Shinohara M, Ueda J (2013) Wearable sensorimotor enhancer for fingertip based on stochastic resonance effect. IEEE Transactions on Human-Machine Systems 43: 333–337.
21. Simonotto E, Riani M, Seife C, Roberts M, Twitty J, et al. (1997) Visual perception of stochastic resonance. Physical Review Letters 78: 1186–1189.
22. Nikitin A, Stocks NG, Morse RP (2007) Enhanced information transmission with signal-dependent noise in an array of nonlinear elements. Physical Review E 75: no.021121.
23. Patel A, Kosko B (2009) Error-probability noise benefits in threshold neural signal detection. Neural Networks 22: 697–706.
24. Bezrukov SM, Vodyanoy I (1997) Stochastic resonance in non-dynamical systems without response thresholds. Nature 385: 319–321.
25. Rousseau D, Rojas-Varela J, Chapeau-Blondeau F (2003) Stochastic resonance for nonlinear sensors with saturation. Physical Review E 67: no.021102.
26. Chapeau-Blondeau F, Rousseau D (2004) Enhancement by noise in parallel arrays of sensors with power-law characteristics. Physical Review E 70: no.060101(R).
27. Blanchard S, Rousseau D, Chapeau-Blondeau F (2007) Noise enhancement of signal transduction by parallel arrays of nonlinear neurons with threshold saturation. Neurocomputing 71: 333–341.
28. Chapeau-Blondeau F, Duan F, Abbott D (2007) Synaptic signal transduction aided by noise in a dynamical saturating model. Physical Review E 81: no.021124.
29. Stocks NG (2000) Suprathreshold stochastic resonance in multilevel threshold systems. Physical Review Letters 84: 2310–2313.
30. Stocks NG (2001) Information transmission in parallel threshold arrays: Suprathreshold stochastic resonance. Physical Review E 63: no.041114.
31. Bulsara AR, Schmera G (1993) Stochastic resonance in globally coupled nonlinear oscillators. Physical Review E 47: 3734–3737.
32. Lindner JF, Meadows BK, Ditto WL, Inchiosa ME, Bulsara AR (1995) Array enhanced stochastic resonance and spatiotemporal synchronization. Physical Review Letters 75: 3–6.
33. Perc M (2007) Stochastic resonance on excitable small-world networks via a pacemaker. Physical Review E 76: no.066203.
34. Benzi R (2009) Stochastic resonance in complex systems. Journal of Statistical Mechanics: Theory and Experiment 1: no.P01052.

35. Perc M (2008) Stochastic resonance on weakly paced scale-free networks. Physical Review E 78: no.036105.
36. Wang Q, Perc M, Duan Z, Chen G (2009) Delay-induced multiple stochastic resonances on scalefree neuronal networks. Chaos 19: no.023112.
37. Gan C, Perc M, Wang Q (2010) Delay-aided stochastic multiresonances on scale-free FitzHugh-Nagumo neuronal networks. Chinese Physical B 19: no.040508.
38. Gosak M, Korošak D, Marhl M (2011) Topologically determined optimal stochastic resonance responses of spatially embedded networks. New Jounral of Physics 13: no.013012.
39. Gosak M, Perc M, Kralj S (2011) Stochastic resonance in a locally excited system of bistable oscillators. The European Physical Journal B 80: 519–528.
40. Teramae J, Tsubo Y, Fukai T (2012) Optimal spike-based communication in excitable networks with strong-sparse and weak-dense links. Scientific Reports 2: no.00485.
41. Hänggi P, Jung P, Zerbe C, Moss F (1993) Can colored noise improve stochastic resonance? Journal of Statistical Physics 70: 25–47.
42. Xu B, Li J, Duan F, Zheng J (2003) Effects of colored noise on multi-frequency signal processing via stochastic resonance with tuning system parameters. Chaos, Solitons & Fractals 16: 93–106.
43. Makra P, Gingl Z, Fülei T (2003) Signal-to-noise ratio gain in stochastic resonators driven by coloured noises. Physics Letters A 317: 228–232.
44. Neiman A, Sung W (1996) Memory effects on stochastic resonance. Physics Letters A 223: 341–347.
45. Inchiosa ME, Bulsara AR (1996) Signal detection statistics of stochastic resonators. Physical Review E 53: R2021–R2024.
46. Kosko B, Mitaim S (2001) Robust stochastic resonance: Signal detection and adaptation in impulsive noise. Physical Review E 64: no.051110.
47. Zozor S, Amblard PO (2003) Stochastic resonance in locally optimal detectors. IEEE Transactions on Signal Processing 51: 3177–3181.
48. Kay S (2000) Can detectabilty be improved by adding noise? IEEE Signal Processing Letters 7: 8–10.
49. Chen H, Varshney PK, Michels JH, Kay SM (2007) Theory of the stochastic resonance effect in signal detection: Part I–fixed detectors. IEEE Transactions on Signal Processing 55: 3172–3184.
50. Chen H, Varshney PK (2008) Theory of the stochastic resonance effect in signal detection: Part II–variable detectors. IEEE Transactions on Signal Processing 56: 5031–5041.
51. Chapeau-Blondeau F, Rousseau D (2009) Raising the noise to improve performance in optimal processing. :Journal of Statistical Mechanics Theory and Experiment 1: no.P01003.
52. Patel A, Kosko B (2011) Noise benefits in quantizer-array correlation detection and watermark decoding. IEEE Transactions on Signal Processing 59: 488–505.
53. Duan F, Chapeau-Blondeau F, Abbott D (2011) Fisher-information condition for enhanced signal detection via stochastic resonance. Physical Review E 84: no.051107.
54. Duan F, Chapeau-Blondeau F, Abbott D (2012) Fisher information as a metric of locally optimal processing and stochastic resonance. PLoS ONE 7: no.e34282.
55. Zeng L, Li J, Shi J (2012) M-ary signal detection via a bistable system in the presence of Lévy noise. Chaos, Solitons & Fractals 45: 378–382.
56. Poor HV (1982) Signal detection in the presence of weakly dependent noise-part I: Optimum detection. IEEE Transactions on Information Theory 28: 735–744.
57. Poor HV (1982) Signal detection in the presence of weakly dependent noise-part II: Robust detection. IEEE Transactions on Information Theory 28: 744–752.
58. Martinez AB, Swaszek PF, Thomas JB (1984) Locally optimal detection in multivariate nongaussian noise. IEEE Transactions on Information Theory 30: 815–822.
59. Portnoy SL (1977) Robust estimation in dependent situations. IEEE Transactions on Information Theory 5: 22–43.
60. Kassam SA (1988) Signal Detection in Non-Gaussian Noise. New York: Springer-Verlag.
61. FitzHugh R (1961) Impulses and physiological states in theoretical models of nerve membrane. Biophysical Journal 1: 455–466.
62. Kay S (1998) Fundamentals of Statistical Signal Processing. New Jersey: Prentice-Hall, Englewood Cliffs.
63. Hänggi P, Inchiosa ME, Fogliatti D, Bulsara AR (2000) Nonlinear stochastic resonance: The saga of anomalous output-input gain. Physical Review E 62: 6155–6163.